Prion Replication Alters the Distribution of Synaptophysin and Caveolin 1 in Neuronal Lipid Rafts

Milene Russelakis-Carneiro,* Claudio Hetz,*† Kinsey Maundrell,* and Claudio Soto*‡

From the Serono Pharmaceutical Research Institute, Geneva, Switzerland; the Instituto de Ciencias Biomédicas,† Universidad de Chile, Santiago, Chile; and the Department of Neurology,‡ University of Texas Medical Branch, Galveston, Texas*

The main event in the pathogenesis of prion diseases is the conversion of the cellular prion protein (PrP^C) into the abnormal, protease-resistant prion protein (PrP^{res}). PrP^C is a GPI-anchored protein located in lipid rafts or detergent-resistant membranes (DRMs). Here we describe the association of PrP with DRMs in neuronal cell bodies and axons during the course of murine scrapie and its relation with the distribution of the PrP-interacting proteins caveolin 1 and synaptophysin. Scrapie infection triggered the accumulation of PrP^{res} in DRMs from retinas and optic nerves from early stages of the disease before evidence of neuronal cell loss. Most of the PrP^{res} remained associated with lipid rafts throughout different stages in disease progression. In contrast to PrP^{res}, caveolin 1 and synaptophysin in retina and optic nerves shifted to non-DRM fractions during the course of scrapie infection. The accumulation of PrP^{res} in DRMs was not associated with a general alteration in their composition, because no change in the total protein distribution across the sucrose gradient or in the flotation characteristics of the glycosphingolipid GM1 or Thy-1 were observed until advanced stages of the disease. However, an increase in total cholesterol levels was observed in optic nerve and retinas. Only during late stages of the disease was a decrease in the number of neuronal cell bodies observed, suggesting that synaptic abnormalities are the earliest sign of neuronal dysfunction that ultimately results in neuronal death. These results indicate that prion replication triggers an abnormal localization of caveolin 1 and synaptophysin, which in turn may alter neuronal function.

Transmissible spongiform encephalopathies or prion diseases are a group of infectious neurodegenerative diseases that affect several species, including humans.[1] The hallmark pathological features of transmissible spongiform encephalopathies are the spongiform degeneration of the brain, accompanied by extensive neuronal loss, synaptic alterations, astrogliosis, and cerebral accumulation of a misfolded and protease-resistant form of the prion protein, termed PrP^{res}.[1,2] In infectious forms of the disease, PrP^{res} formation from wild-type PrP^C is initiated by exposure to the exogenous infectious agent, which promotes a conformational transition from α-helical to β-sheet structure, resulting in the formation of PrP^{res}.[3] Although the nature of the infectious agent has not been completely elucidated, PrP^{res} seems to be the main constituent. Based on studies using neuronal cell lines as a model, prion replication was suggested to occur either at the cell surface or during the endocytic trafficking of PrP^C.[4–6] *In vivo*, PrP^{res} has been identified in lysosome-related structures as well as in the neuronal plasmalemma and in extracellular amyloid deposits in human and experimental prion diseases.[7]

PrP^C is constitutively expressed in neurons as a GPI-anchored protein and, like other members of this class, it is localized into the cholesterol and sphingolipid-rich domains of the plasma membrane, termed lipid rafts. These lipid domains are defined biochemically by their insolubility in nonionic detergents at low temperature and thus are also termed detergent-resistant membranes (DRMs).[8] A closely related membrane fraction termed caveolae-rich domains referring to the presence of the structural protein caveolin 1.[6,9]

In neurons, lipid rafts provide a platform for signal transduction initiated by several classes of neurotrophic factors.[10] The high concentration of receptors and other signaling molecules in DRMs provided a first hint of a potential role of PrP^C in signal transduction and further experimental support for this idea came from antibody-

Address reprint requests to Dr. Claudio Soto, Department of Neurology, University of Texas Medical Branch, 301 University Blvd., Galveston, TX 77555. E-mail: clsoto@utmb.edu.

mediated cross-linking experiments showing a caveolin 1-dependent coupling of PrP^C to Fyn, a member of the Src family of tyrosine kinases.[11] Caveolin 1 has been shown to be essential in the regulation and formation of signaling complexes in rafts because it acts as a scaffold protein modulating the localization of diverse signaling proteins in this plasma membrane subdomain.[8] Furthermore, several proteins implicated in neuronal signaling interact directly with PrP^C including caveolin 1, synaptophysin, and others.[12,13] Because PrP^C has been shown to promote the activation of neuroprotective signaling pathways, it is likely that the subcellular localization of PrP^C may be crucial for its normal function.[12–14]

The formation of PrP^{res} induces neuronal cell dysfunction although the mechanism by which this occurs remains unclear and controversial.[14] We have shown recently that low concentrations of purified PrP^{res} induce neuronal apoptosis via the endoplasmic reticulum stress pathway leading to activation of caspase-12.[15] Other laboratories have demonstrated that prion infection promotes early alterations in synaptic function before neuronal death is observed.[16,17] This phenomenon is accompanied by a decreased expression of crucial proteins involved in exocytosis and neurotransmission, such as synaptophysin, SNAP-25, synapsins, and others in brains of both scrapie-infected mice and humans affected with Creutzfeldt-Jacob disease.[18] The association of PrP^C and PrP^{res} with DRMs appears to play an important role in prion propagation and disease pathogenesis. For example, pharmacological treatments that modify the lipid composition of the DRMs either by decreasing cholesterol levels or increasing sphingolipid levels, result in decreased efficiency of prion propagation in N2a cells infected with scrapie.[19–21] In addition, recombinant transmembrane PrP^C lacking the GPI anchor is not located in DRMs and acts as a poor substrate for the formation of PrP^{res} in neuroblastoma cells and in a transgenic mice model.[20] *In vitro* studies using a cell-free system have shown that the insertion of PrP^{res} into the DRMs is required for the conversion of PrP^c into PrP^{res}.[22] Finally, the modification of cholesterol levels has a direct impact on the toxic effect of brain-derived PrP^{res} *in vitro*.[21] Taken together, these data indicate that lipid rafts are essential plasma membrane subdomains required for the process of prion replication and for its pathogenic effects on neuronal function.

Most experiments performed *in vivo* on the accumulation of PrP^{res} in DRMs have focused on the terminal stages of scrapie in hamsters.[9] However, it is not known whether the DRM is a site for PrP^{res} formation, and furthermore, the effect of PrP^{res} replication on DRM integrity and on the activity of other DRM-associated proteins is unclear. In this paper, we have studied the association of PrP^C and PrP^{res} with DRMs from the early stages of scrapie infection onwards, and we have compared these results with the distribution of other key raft-associated proteins, in particular synaptophysin and caveolin 1, which are important for neuronal activity. As a further goal of this study we wished to distinguish between the effects on neuronal cell bodies as compared to axons, and for this we have focused on the visual system, in which the retina and optic nerve can be taken as representative of neuronal cell bodies and axons, respectively. Our data show that, in noninfected mice, PrP^c, synaptophysin, and caveolin 1 are all present in DRMs from both cell bodies and axons. At early stages after infection with prions, before neuronal loss was apparent, PrP^{res} was detected in DRMs from cell bodies and axons while synaptophysin and caveolin 1 were rapidly detectable in non-DRM fractions. No changes in the distribution of other components of DRMs, such as GM1 and the GPI-anchored protein Thy-1, were observed, indicating that the accumulation of PrP^{res} in DRMs does not drastically alter these membrane subdomains. Our results reveal for the first time that the accumulation of the misfolded PrP^{res} protein in lipid rafts *in vivo* may alter the localization of proteins essential for neuronal function, and this may contribute to neuronal death and neurological defects characteristic of later stages of the disease.

Materials and Methods

Animals

C57BL/6J mice from both sexes were used in the experiments. Mice were housed in a temperature- and humidity-controlled environment and had free access to food and water. All experiments were performed according to the Swiss guidelines for animal experimentation.

Stereotaxic Injection

Groups of mice were injected stereotaxically in both right and left superior colliculus with 1 μl of 10% brain homogenate prepared from normal brains or from terminally ill ME7- or 139A-infected mice. A further group of animals was uninjected. Animals were age-matched at the time of injection. Alternatively, C57BL/6J mice were injected stereotaxically in the hippocampus with 1 μl of a 10% brain homogenate taken from mice infected with 139A scrapie at a terminally ill stage. Onset of the clinical disease was measured weekly by determination of body weight loss and decrease in muscle strength using a grid system as described previously.[15]

Clinical Evaluation

Mice were observed for the appearance of clinical signs of scrapie such as ruffling fur, hunched posture, reduced muscle strength, and loss of weight. The first clinical signs of scrapie after injection in superior colliculus were observed at ~20 weeks after infection. Three weeks later, animals showed an increase in the severity of the clinical signs and were sacrificed after a lethal injection of pentobarbital. Animals injected with ME7 or 139A showed similar disease progression. For intrahippocampal injection, the first clinical signs of the disease were observed after 16 weeks of infection. Animals were perfused with heparinized saline solution and brain, optic nerves, and retina were dissected and frozen in dry ice.

DRM Isolation

Tissues were homogenized on ice in 100 μl of phosphate-buffered saline (PBS) containing protease inhibitors (Roche) and 0.1% Triton X-100. Samples were left on ice for 30 minutes then mixed with 2 vol of 60% w/v sucrose in PBS before being loaded into the bottom of ultracentrifuge tubes (TLA 100.2; Beckman Instruments). A stepwise sucrose gradient consisting of 700 μl of 35% w/v and 150 μl of 15% w/v sucrose solution in PBS was carefully overlaid above the sample and the tubes were centrifuged at 150,000 × *g* for 18 hours at 4°C. After centrifugation, nine fractions of 100 μl each were carefully collected from the top of the gradient. For Western blotting analyses, 20 μl of each of these fractions were used to load in the gel. The material present in the pellet was resuspended in 1% Triton X-100 solution and homogenized by sonication on ice using a probe sonicator. All procedures were performed at 4°C. DRMs are defined here as the fraction that floats into the 15% sucrose layer.

Proteinase K (PK) Digestion

To identify PrP^{res}, PK digestion was performed at 37°C for 30 minutes using 0.25 μg of PK (Boehringer-Mannheim) per 10 μg of total protein. PK digestion on DRM samples or on whole homogenate from retinas and optic nerves was performed in buffer containing 0.5% Triton X-100 and 0.05% sodium dodecyl sulfate.

Subcellular Fractionation

Retinal tissue was homogenized in a buffer containing 8% sucrose (w/v), 20 mmol/L HCl-Tricine, pH 7.8, 1 mmol/L ethylenediaminetetraacetic acid. After a first spin at 2000 × *g* for 5 minutes to eliminate the unbroken tissue and nuclei, the supernatant was centrifuged at 100,000 × *g* for 30 minutes. Supernatant and pellet from the 100,000 × *g* centrifugation represent the cytosolic and the membrane fractions, respectively. Protein of each fraction were solubilized in loading buffer and analyzed by Western blotting.

Western Blot Procedure

Proteins present in 20 μl of each fraction from the flotation gradient were separated by sodium dodecyl sulfate-polyacrylamide gel electrophoresis (precast 10% NuPage Tris-Bis gel; Invitrogen), and transferred to nitrocellulose membranes. Membranes were blocked in 5% nonfat milk for 1 hour at room temperature and then incubated in PBS containing 0.3% Tween 20 and one of the following primary antibodies: 6H4 anti-PrP (1:10,000; Prionics), anti-caveolin 1 (1:5000; BD Transduction Laboratories), anti-β-tubulin isotype (1:1000; Sigma), anti-synaptophysin (1:1000, Sigma), recombinant aerolysin and anti-aerolysin (1:1000; Protox Biotech). Membranes were incubated with the primary antibody for 2 hours at room temperature or overnight at 4°C. Immunoreactivity was revealed using a peroxidase-conjugated secondary antibody (1:5000; Amersham) and enhanced chemiluminescence (Amersham). In some cases, gels were stained with Silver Express (Amersham) to study the overall distribution of protein in different fractions after Triton X-100 extraction.

GM1 Detection

To detect cell surface ganglioside GM1 in the gradient fractions, we used its specific ligand cholera toxin B (CTXB) conjugated with peroxidase (Calbiochem). One μl and 2 μl of each fraction from optic nerve and retina were spotted onto a nitrocellulose membrane. Membranes were blocked for 45 minutes with 3% bovine serum albumin in PBS and then incubated for 1 hour at room temperature, with CTXB diluted to a final concentration of 2 ng/ml in PBS.

Cholesterol Quantification

Total extracts were prepared in PBS 1% Triton X-100 and homogenized by sonication. Nondisrupted tissue was removed by centrifugation and total protein was determined. Cholesterol levels were analyzed using the Kitachi 902 automatic analyzer (Boehringer-Mannheim), using the Cholesterol-Hitachi kit. The percentage of cholesterol related to the total protein content was calculated in control and scrapie-infected samples.

Densitometric Analysis

The amount of protein in each fraction of the gradient was calculated in silver-stained gels using SigmaGel software after scanning. Similar analyses were performed to quantitate signals generated by Western blotting and immunodetected bands were then normalized to total protein in each fraction of the gradient. The results show the mean ratios obtained in at least three animals per group. In the case of the PrP^{res} analyses, the PrP signal obtained after PK digestion was compared to that obtained with the same sample before PK digestion, considered as 100%. Statistical analyses were performed using Student's *t*-test with $P < 0.05$ considered significant.

Analysis of Retinal Ganglion Cells

To quantify the number of neurons in the retinal ganglion cell layer, whole retinas were dissected from the eye under a dissecting microscope, flattened with the vitreous surface up on gelatinized slides and stained with cresyl violet. Retinal areas were measured before and after the staining and tissue retraction was calculated. Only retinas with shrinkage less than 12% were included in the analysis. The retinal ganglion cells are the only cell type in the retinas bearing axons that constitute the optic nerve. The cell bodies of these neurons are located in a specific layer of the retina termed the retina ganglion cell layer. For this reason, neurons were only quantified in this layer. Counts were performed in a square of 55 μm × 55 μm located in three different fields at 1.4 mm temporal,

nasal, and inferior to the optic nerve head in control and ME7 retinas. Quantitative analyses were performed at 20 weeks after injection and at advanced stages of the disease. The results represent the mean of neurons counted in four different retinas from control and infected mice. The criteria for the identification of ganglion cells, amacrine cells, and glia in the ganglion cell layer of rodents was described in detail in previous studies.[23] Cells were counted at a magnification of ×1000. Student's *t*-test was used to analyze the results obtained in the neuronal counts and values of $P < 0.05$ were taken as significant.

Nomenclature

PrP refers to the total amount of the protein before PK digestion whereas PrP^{C} and PrP^{res} refer, respectively, to the sensitive and protease-resistant PrP. In the present model, early stages of the disease are considered as survival times before the onset of clinical signs of scrapie and neuronal cell death in the retina. Advanced stages of the disease are considered as survival times in which clinical signs of scrapie are severe and neuronal loss is detectable in retina.

Results

PrP Accumulates in DRMs from Neuronal Bodies at Early Stages of Scrapie Infection

The distribution of PrP was studied in retinas and optic nerves at different times after injection with ME7 or 139A prions into the superior colliculus, one of the main target areas of the retina. In retinas from noninfected mice, the majority of the di- and mono-glycosylated forms of PrP was present in DRMs (Figure 1A, fraction 1), while a minor proportion was also detected in the less bouyant fractions (Figure 1A; fractions 2, 3, and 4). The nonglycosylated form of PrP was not detected in retinas from control animals as described previously (Figure 1A).[24] Infection with either ME7 or 139A gave similar results. In retinas, in addition to the di- and mono-glycosylated forms of PrP, the nonglycosylated form appears as shown previously.[24] Total PrP associated with the DRM fraction is significantly higher in infected mice at 15 and 20 weeks after inoculation (Figure 1, A and C; fraction 1). The majority of PrP at 15 and 20 weeks after injection is associated with DRMs, although a minor component of the protein is seen in fractions 2, 3, 4, and 5 of the gradient (Figure 1A). A change in the PrP distribution is observed at advanced stages of scrapie probably reflecting the disruption of membranes in dying neurons, as described later in this section.

In optic nerves from control mice, the di-, mono-, and nonglycosylated forms of PrP are found in the DRMs, with a minor amount of this protein located in fraction 2, 3, and 4 of the gradient (Figure 1B). The quantity of PrP in DRMs when normalized to the total protein in this fraction is approximately fourfold lower in optic nerves as compared to retina (Figure 1, C and D). After injection of scrapie, no

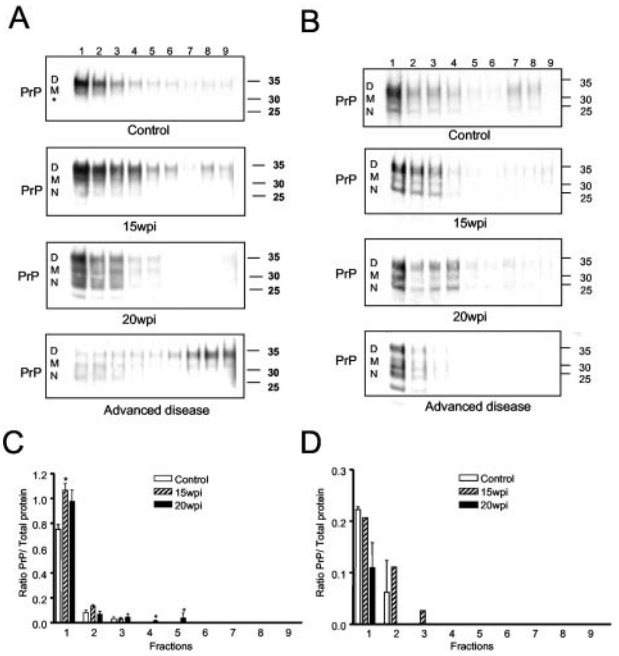

Figure 1. Accumulation of PrP in DRMs from retinas and optic nerves at early stages of prion disease in mice. The distribution of PrP along buoyant sucrose gradient after Triton X-100 extraction at different times after scrapie infection was analyzed in retinas (**A**) and optic nerves (**B**) by Western blotting. The ratio between the PrP-immunoreactive signal and the total protein concentration in each fraction was calculated at different times after infection in retinas (**C**) and optic nerves (**D**). D-, M-, and N- correspond to the di-, mono-, and nonglycosylated forms of PrP, respectively. wpi, weeks postinjection. Data were statistically analyzed by Student's *t*-test; *, $P < 0.05$.

significant change in the distribution of PrP in axons was observed at any time during the course of the disease (Figure 1, B and D). Quantitative analyses also showed no significant accumulation of PrP in DRMs or in any other fraction of the gradient (Figure 1D). Thus, the accumulation of PrP in this system occurs mainly in neuronal cell bodies.

The characteristic feature of prion diseases is the presence of the protease resistant form of PrP, which accumulates in brain tissue.[3] We therefore quantified the PrP^{res} component from DRMs and total homogenates of retinas and optic nerves by PK digestion followed by Western blotting analyses. PrP^{res} was detected in DRMs from both retinas and optic nerves from 15 weeks onwards, although it was much more abundant in the cell bodies (Figure 2A). We quantified the proportion of PrP^{res} with respect to total PrP by densitometric analysis using whole homogenates from retinas and optic nerves at 15 weeks after injection, 20 weeks after injection, and at advanced stages of scrapie. In retinas, ~70% of the PrP detected was in the protease-resistant form, whereas in optic nerves only ~30% of the PrP was protease resistant (Figure 2B), again suggesting that the accumulation of PrP^{res} occurs mainly in cell bodies.

DRM Properties Are Preserved during Early Stages of Scrapie Infection

To analyze the protein distribution along the gradient, the proportion of total proteins in each fraction was calcu-

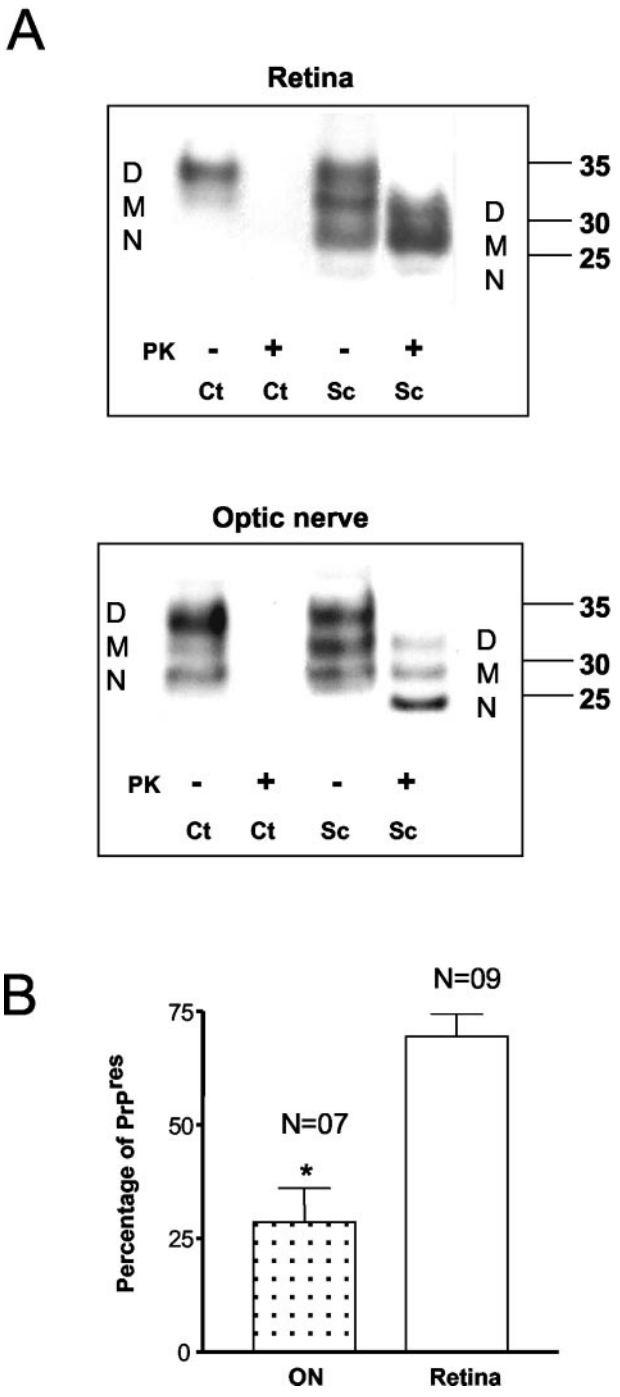

Figure 2. PrP^{res} in retinas and optic nerves. **A:** Western blot showing the PrP profile in retina (**top**) and optic nerve (**bottom**) before and after PK digestion in control (Ct) and scrapie-infected animals (Sc). **B:** The graph illustrates the proportion of PrP after PK digestion (PrP^{res}) related to the amount of total PrP before digestion, considered as 100%, in retinas and optic nerves (ON). D-, M-, and N- correspond to the di-, mono-, and nonglycosylated forms of PrP. Data were statistically analyzed by Student's *t*-test; *, $P < 0.05$.

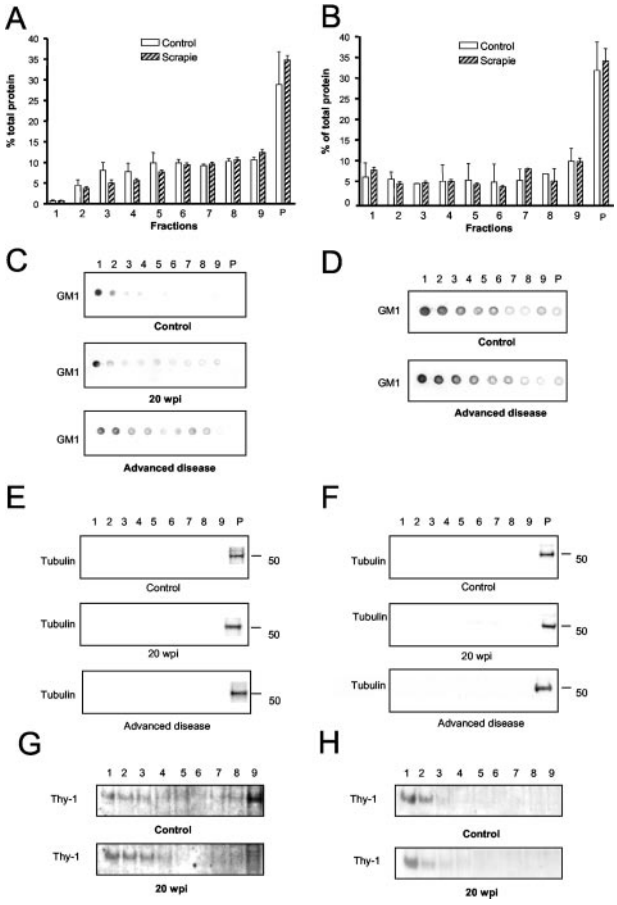

Figure 3. Distribution of total proteins, GM1, tubulin, and Thy-1 in retinas and optic nerves after 0.1% Triton X-100 extraction. Total protein content in different fractions of the sucrose gradient was measured by silver staining of the gels from samples obtained from retinas (**A**) and optic nerves (**B**) of controls and scrapie-infected animals at advanced stages of the disease. None of the differences was statistically significant, as evaluated by Student's *t*-test. The distribution of the DRM-resident ganglioside GM1 was measured by dot blotting in different fractions of samples from retina (**C**) and optic nerve (**D**). The distribution of tubulin and Thy-1 were also studied in samples from retina (**E** and **G**) and optic nerve (**F** and **H**).

lated in silver-stained gels (Figure 3, A and B). In retinas from disease-free mice, less than 1% of the proteins was located in DRMs (Figure 3A). The amount of protein was higher in the less bouyant fractions while the majority of protein was retrieved in the pellet. After infection, a similar protein distribution was found in retinas, even at advanced stages of disease (Figure 3A). In optic nerves, ~5% of total protein was located in DRMs and a similar proportion was found dispersed throughout the gradient, with the majority of the protein being recovered in the pellet (Figure 3B). Again, no changes in the protein distribution along the gradient were observed in scrapie-infected animals. Thus, the presence of PrP^{res} in DRMs seems not to affect the overall distribution of total protein throughout different fractions of the gradient.

To characterize further our DRM preparations, we studied the distribution of the DRM-resident glycolipid GM1, and of the non-DRM-bound protein, tubulin. In retinas from noninfected mice, GM1 was detected almost exclusively in DRMs (Figure 3C). At early stages of the disease (15 and 20 weeks after injection), the distribution of GM1 in retinas remained similar to controls, but at advanced stages, GM1 reactivity was spread throughout the gradient (Figure 3C), most likely reflecting the overall lipid-raft disruption caused by neuronal death. In control optic nerves, GM1 was more broadly distributed along the gradient and no changes were observed at any time

Table 1. Analysis of Total Cholesterol Levels in Retinas, Optic Nerve, and Cortex of 139A Scrapie-Infected Mice

Sample	Cholesterol (mmol/mg protein)		% from control
Retina			
Control	122 ± 24	(n = 3)	
15 wpi	117 ± 8	(n = 3)	−5%
20 wpi	134 ± 2	(n = 3)	10%
Optic nerve			
Control	612 ± 118	(n = 2)	
15 wpi	798 ± 46	(n = 4)	30%*
Cortex			
Control	518 ± 45	(n = 6)	
12 wpi	635 ± 50	(n = 3)	22%*
20 wpi	757 ± 67	(n = 3)	46%†
23 wpi	779 ± 62	(n = 3)	50%†

Data was normalized by the total protein content.
*, $P < 0.05$; †, $P < 0.005$.
wpi, weeks postinjection.

during the course of the disease (Figure 3D). In retinas and optic nerves from control and infected mice, tubulin was consistently detected in the pellet fraction at all survival times studied (Figure 3, E and F). The distribution of other GPI-anchored proteins remained similar in controls and scrapie-infected mice, as judged by the distribution of Thy-1 (Figure 3, G and H) and other GPI-anchored proteins detected using aerolysin-binding overlay assay (data not shown). These findings indicate that the accumulation of PrP^{res} in DRMs observed in retinas at early stages of the disease was not associated with changes in the overall distribution of proteins or with a drastic perturbation in the biochemical characteristics of DRMs.

Cholesterol is one of the principal constituents of lipid rafts[25] and it has been shown to participate in the process of prion replication.[20,21] To analyze the effect of prion infection on cholesterol metabolism, total cholesterol levels were analyzed in retinas and optic nerve samples from control and scrapie-infected mice. In retina, a small increase in total cholesterol level was observed after 20 weeks of infection (Table 1). However, early changes were detected in the optic nerve of scrapie-infected mice, in which an increase of 30% in total cholesterol levels at 15 weeks after injection was observed (Table 1).

Alterations in Caveolin 1 and Synaptophysin Subcellular Distribution during Early Stages of Scrapie

Caveolin 1 is an important component of the caveolae-type DRMs and plays many essential functions,[26] including some reported interactions with PrP.[27] Therefore, we decided to study whether the distribution of caveolin 1 is altered in retinas and optic nerves in scrapie-infected mice. In retinas from control mice, caveolin 1 is found in DRM and non-DRM fractions (Figure 4A; fractions 1, 2, 3, 9). In scrapie-infected retinas the majority of caveolin 1 was detected in lower, mostly intermediate fractions (Figure 4A, fractions 5 and 6) from 15 weeks onwards. This occurred concomitantly with a progressive decrease of caveolin 1 in DRMs and at 20 weeks after injection, only a minor proportion of this protein was detected in retinal DRMs. In retinas at advanced stages, caveolin 1 was present in lower fractions of the gradient (Figure 4A, fractions 8 and 9) and it was no longer detected in the DRM fraction. A 57% and 76% reduction of the amount of caveolin 1 present in rafts was observed at 15 and 20 weeks after injection, respectively (Figure 4C). Despite the changes in the distribution of caveolin 1, the overall levels of the protein remained similar at 15 and 20 weeks after injection compared to those observed in control animals (Figure 4E).

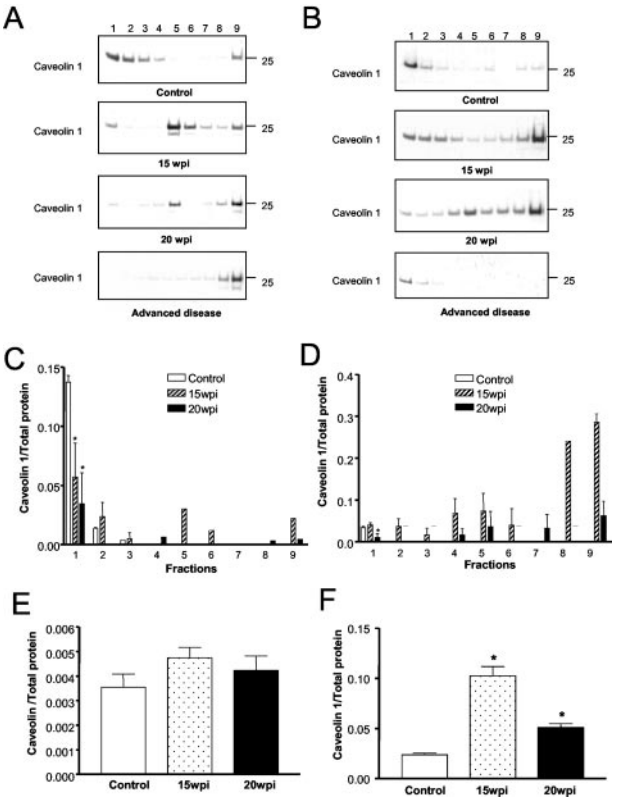

Figure 4. Dissociation of caveolin 1 from DRMs in retinas and optic nerves during scrapie infection in mice. Distribution of caveolin 1 along the sucrose gradient after Triton X-100 extraction at different times after scrapie injection in retinas (**A**) and optic nerves (**B**). The ratio between the amount of caveolin 1 and total protein in each fraction was calculated at different times after infection in whole homogenates from retinas (**C**) and optic nerves (**D**). Also, the ratio between the total amount of caveolin 1 and the total amount of proteins in retinas (**E**) and optic nerves (**F**) was calculated. Data were statistically analyzed by Student's t-test; *, $P < 0.05$. wpi, weeks postinjection.

In optic nerves from disease-free mice, caveolin 1 was found mostly in DRMs (Figure 4B). After prion infection, caveolin 1 was detected in almost every fraction of the gradient at 15 and 20 weeks after injection, although the majority of this protein was located in fraction 9 (Figure 4, B and D). This occurred in parallel with an increase in the total concentration of caveolin 1 in axons (Figure 4F). At 20 weeks, a decrease of this protein in DRMs was detected (Figure 4F) although the overall levels of caveolin 1 remained slightly elevated compared to control animals, but lower than those seen at 15 weeks after injec-

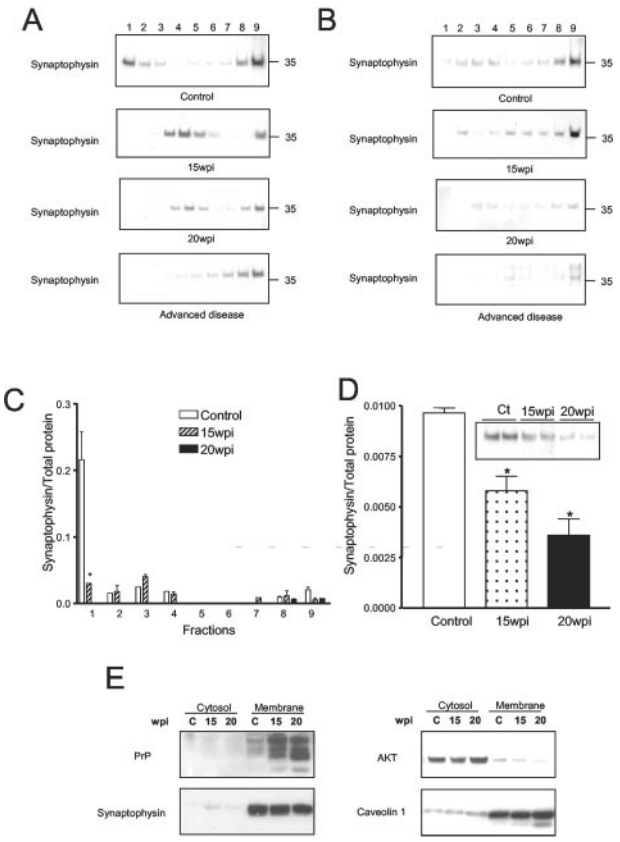

Figure 5. Dissociation of synaptophysin from DRMs in retinas during scrapie infection in mice. Synaptophysin distribution along the buoyant sucrose gradient after Triton X-100 extraction at different survival times after scrapie infection in retinas (**A**) and optic nerves (**B**). **C:** The ratio between the amount of synaptophysin and total protein in each fraction was calculated at different times after infection. **D:** The ratio between the total amount of synaptophysin and the total amount of proteins in retinas was calculated. The **inset** shows Western blotting of synaptophysin in controls and scrapie-infected mice at different survival times. Data were statistically analyzed by Student's *t*-test; *, $P < 0.05$. **E:** Western blotting from retina (**left**) and optic nerve (**right**) after cytosol and membrane separation in the absence of detergent.

tion (Figure 4F). At advanced stages, caveolin 1 was detected at very low levels and mostly in DRMs (Figure 4, B and D).

Another DRM-associated protein that plays an important function in neuronal biology is synaptophysin,[28] which has also been implicated in prion diseases. A decrease in the synaptophysin expression and synaptic dysfunction are the earliest pathological changes that have been described in prion diseases.[29] For this reason, the distribution of synaptophysin was studied in scrapie-infected and control mice. In retinas from disease-free mice, the majority of synaptophysin was found in DRMs as well as in the lowest fraction of the gradient (Figure 5A, fractions 1 and 9), with small amounts being detected in intermediate fractions (Figure 5, A and C). Fifteen weeks after injection of scrapie, the distribution of synaptophysin was altered with the majority being located in intermediate and lower fractions of the gradient (Figure 5, A and C; fractions 3, 4, 5, and 9). At 20 weeks after injection, synaptophysin was no longer detectable in DRMs but was present exclusively in intermediate and lower fractions of the gradient (Figure 5, A and C; fractions 3, 4, 5, 8, and 9). At advanced stages, this protein was found only at the lowest fractions of the gradient (Figure 5, A and C; fractions 7, 8, and 9). In addition, synaptophysin levels were significantly lower from 15 weeks after injection onwards (Figure 5D). Similar alterations were observed in the optic nerve (Figure 5B).

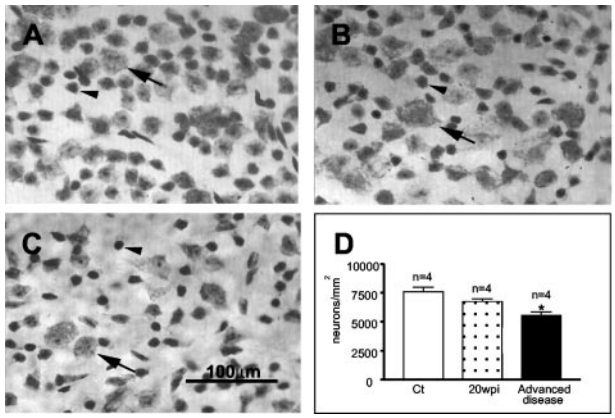

Figure 6. Degeneration of retinal ganglion cells at advanced stages of scrapie. The photomicrographs illustrate the retinal ganglion cell layer in flat-mounted retinas stained by cresyl violet. **A:** Control mice. **B:** Retina from mice at 20 weeks after infection. **C:** Retina from mice at advanced stage of the disease. **D:** Graph illustrating the number of neurons per mm^2 in the retinal ganglion cell layer after prion infection. The **arrows** indicate the retinal ganglion cells and the **arrowheads** indicate the displaced amacrine cells. Data were statistically analyzed by Student's *t*-test; *, $P < 0.05$.

To analyze whether the changes on subcellular distribution of caveolin and synaptophysin are because of detachment from the membranes, homogenates from infected retinas were separated into cytosol and total membranes in the absence of detergents. The distribution of AKT was followed as a marker for cytosolic proteins (Figure 5E). Analysis of the distribution of PrP, caveolin 1, and synaptophysin in this preparation indicated that each of these proteins located to the membrane fraction before or after scrapie infection. These results show that the changes in the distribution of these proteins in the sucrose gradient are not a consequence of their dissociation from the membranes (Figure 5E), indicating that they either moved out of the lipid raft fraction or that they are located in different types of rafts with distinct properties in sucrose gradient experiments.

Loss of Neurons in the Retinal Ganglion Cell Layer Occurs Only at Advanced Stages of Scrapie

We studied whether the changes in the protein composition of DRMs in retinas were associated with neuronal loss in the retinal ganglion cell layer at 20 weeks after injection and at advanced stages of scrapie. The analyses were performed in the retinal layer because it contains the cell bodies from the axons located in the optic nerve. No significant differences in the neuronal density were observed in the retinal ganglion cell layer from control and ME7-injected mice at 20 weeks after injection (Figure 6, A and B). At advanced stages of scrapie, the loss of neurons with large cell bodies, corresponding to

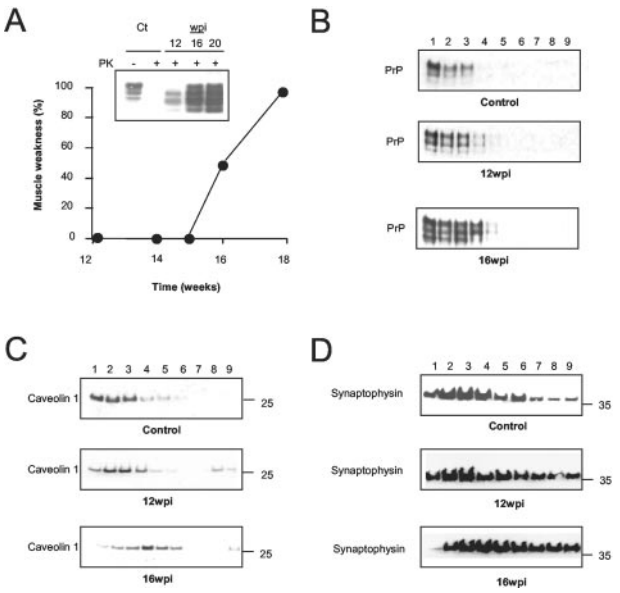

Figure 7. Altered distribution of caveolin 1 and synaptophysin in the cortex of scrapie-infected mice. **A:** Eight animals per group were injected in the hippocampus with 1 μl of 10% brain homogenate from normal (Ct) or 139A scrapie-infected mice. Muscle strength was determined by measuring the time during which animals were able to cling to an inverted grill. Values represent the percentage of animals in each group that fell within 1 minute after inversion. **Inset**: Western blot analysis of PrP^{res} in PK-digested cortex brain homogenates from infected animals at 12, 16, and 20 weeks after injection. In cortex brain homogenates PrP (**B**), caveolin 1 (**C**), and synaptophysin (**D**) distribution along the buoyant sucrose gradient after Triton X-100 extraction at different survival times after scrapie infection.

the retinal ganglion cells in this layer, was apparent (Figure 6, A and C). A reduction of ~25% in the density of neurons was observed in the retinal ganglion cell layer of retinas from scrapie mice, as compared with controls (Figure 6D; analysis of variance, $P < 0.05$). It should be noted that in rodents ~40 to 50% of the neurons in the retinal ganglion cell layer are amacrine cells or interneurons (also counted in our preparations).[23] As illustrated in Figure 6C, these cells seem to be spared from death even at advanced stages of scrapie. Thus, a 25% decrease in neurons in the retinal ganglion cell layer is likely to represent an ~50% reduction in the number of retinal ganglion cells.

Alterations in Caveolin 1 and Synaptophysin Subcellular Distribution in the Brain of Scrapie-Infected Mice

To confirm our results obtained using the visual system, a series of mice were also infected by intrahippocampal injection of 139A scrapie-infected brain extract. Analysis of disease progression revealed that this route of infection leads to the appearance of the first clinical signs after 16 weeks after injection (Figure 7A). As described above in scrapie-infected retinas, PrP^{res} accumulation was detected during the presymptomatic phase of the disease at 12 weeks after injection (Figure 7A, inset). Changes in the proportion of the di-, mono-, and nonglycosylated forms and an accumulation of PrP in DRMs were also observed from 12 weeks onwards (Figure 7B). In addition, caveolin 1 distribution along the sucrose gradient was affected by prion infection early in the disease progression (Figure 7C). A decrease in synaptophysin in the DRM fraction was also detected concomitant with an increase of this protein in more dense fractions of the gradient (Figure 7D). Finally, quantification of total cholesterol level in the brain of scrapie-infected animals, revealed a progressive increase of total cholesterol (Table 1), thus corroborating our results obtained using retinas and optic nerves.

Discussion

The complexity of the types and biochemical composition of neuronal cells in the brain has complicated analyses of the impact of prion replication on neuronal function. In an attempt to circumvent this problem, in this report we have used the visual system of the rodent as a model for prion infection. In this system, the retina is made up almost entirely of the cell bodies of the retinal ganglion cells, and the optic nerve comprises the axons of these cells. More than 90% of the axons of the retinal ganglion cells project to the superior colliculus.[30] This neuronal network forms an integral part of the central nervous system. It is possible to induce prion pathology in the visual system by stereotaxic injection into the superior colliculus and all of the typical features of the disease can be reproduced in this model.[31] By dissecting the retina from the optic nerve, we have been able to investigate independently the effects of prion infection on neuronal cell bodies and axons.

Lipid rafts or DRMs are membrane subdomains rich in proteins implicated in signal transduction and thus the correct structural organization and composition of DRMs is essential for normal cellular functioning.[8] PrP^{C} has been described as a lipid raft-resident protein and PrP^{res} was detected in DRMs of infected N2a cells and also in the brains of Syrian hamsters infected with scrapie.[6,9] The association of PrP with DRMs is believed to play a crucial role in the conversion of PrP^{C} into PrP^{res} although little is known about this association in the brain during the progression of prion diseases. Interestingly, experimentally modifying the levels of cholesterol[20,21] or sphingomyelin,[19] the two principal lipid components of the lipid rafts, has been shown to dramatically alter the efficiency of prion replication in chronically infected N2a cells. These results have shown that decreasing the content of cholesterol in the raft prevents PrP^{res} replication in N2a cells chronically infected with scrapie, while depleting sphingomyelin increases PrP^{res} formation in this experimental system. Furthermore, pharmacological modification of cholesterol levels in lipid rafts has a direct impact in the neurotoxic activity of PrP^{res} *in vitro*.[21] Thus, lipid rafts appear to be essential subcellular compartments involved in the propagation and pathogenesis of PrP^{res}. The major goal of this study was to investigate the impact of PrP^{res} replication on the biochemical characteristics of DRMs and the association with proteins essential for normal neuronal functions.

DRMs are defined here as the membrane fraction that resists to 0.1% Triton X-100 extraction at 4°C and floats into a 15% layer of a sucrose gradient. In this report DRMs were characterized by the presence of PrP, a second GPI-anchored protein Thy-1, caveolin 1, and the raft-resident ganglioside GM1. In disease-free mice, most of PrP^C is located in DRMs of cell bodies whereas only a minor fraction is located in axons. After injection of scrapie into the superior colliculus, a significant and progressive accumulation of PrP, particularly its nonglycosylated form, was observed in DRMs from retinas before any indication of neuronal cell death or clinical signs of the disease were detected. No significant increase in PrP levels in the DRMs from optic nerve was detected at any time during the course of the disease. These results indicate that the DRMs from neuronal cell bodies are the preferential site for the formation of PrP^{res} in the central nervous system.

The involvement of DRMs in the conversion of PrP^c into PrP^{res} has been extensively studied during advanced stages of scrapie infection in the hamster.[9] Here we describe for the first time that PrP^{res} accumulates in DRMs during early stages of the disease, well before detectable signs of neuronal death. To extend these observations, we also examined the effect of prion replication on the distribution of two other key proteins, caveolin 1 and synaptophysin. Caveolin 1 is an essential structural protein required for formation of caveolae, the lipid raft structures in which PrP has been described. Within these structures, caveolin 1 appears to act as a scaffold protein that organizes membrane receptors, kinases, GTPases, and others and it is necessary for the initiation of signal transduction.[32] Synaptophysin plays a major role in the formation of synaptic vesicles, and a decrease in synaptophysin levels and synaptic function are the earliest neuronal changes observed in the brain of mice infected with prions.[16] In addition, decreased expression of synaptophysin, synapsins, syntaxins, SNAP-25, and Rab3a, proteins involved in exocytosis and neurotransmission, occurs in the brain of human patients affected with Creutzfeldt-Jakob disease.[18] Our findings also point to a gradual decrease on the concentration of synaptophysin during the disease progression. Conversely, the levels of caveolin are increased during the disease, especially in axons. The formation of signaling complexes in lipid rafts involving caveolin 1 and synapsis-related proteins is involved in the process of synaptic potentiation[33] and recent data point to synapses as principal targets of abnormal PrP deposition. Indeed, loss of synapses is an early abnormality in experimental scrapie.[16]

The mechanism by which PrP^{res} formation is associated to synaptic dysfunction in prion diseases remains unclear although different possibilities have been discussed, including loss of the neuroprotective function of PrP^C caused by the conversion into PrP^{res}[12] or alteration in normal neuronal excitability and synaptic transmission.[34] In this study we provide evidence for a further possibility namely that the presence of PrP^{res} in lipid rafts affects the normal subcellular location of caveolin 1 and synaptophysin, thus leading to abnormal neuronal signaling and synaptic dysfunction. Alteration in the distribution of caveolin 1 and synaptophysin along the sucrose gradient after Triton X-100 extraction was observed before neuronal death, detected by the decrease in the number of neurons in the retinal ganglion cell layer. This suggests that synapse dysfunction is contributing rather than being a consequence of neuronal death, here defined as a decrease in the density of neurons.

How scrapie infection triggers an abnormal distribution of caveolin 1 and synaptophysin remains to be determined. Interestingly, no change in the distribution of another GPI-anchored protein, Thy1, was observed during this period. One possible mechanism could be because of a modified interaction between PrP^{res} and caveolin1/synaptophysin that alters insertion of these proteins into the lipid raft. Alternatively, an indirect effect of PrP^{res} on the lipid raft may occur. Previous reports indicated that the infection of N2a cells with scrapie decreased the fluidity of the plasma membrane resulting in an abnormal response to stimuli that induced calcium signaling.[35] Our findings showing an increase on cholesterol concentration in membranes during scrapie, provide support for this concept. In addition, altered lipid composition has been previously reported in the brain of scrapie-infected mice.[36] In this context, recent data pointing to heterogeneity within the lipid raft fraction in which it was shown that Thy-1- and PrP-containing DRMs differ markedly from each other in terms of their lipid composition[37] may explain the differential effects we observe on the distribution of these two proteins after scrapie infection. Moreover, Triton X-100 extraction at 37°C was shown to result in the separation of PrP^C and PrP^{res} into two distinct peaks of different densities after centrifugation in sucrose gradients. Thus the evidence increasingly points to the existence of microheterogeneity of lipid rafts, and similar conclusions were also described recently in cerebellar granule cells.[38]

The localization of different proteins to particular lipid rafts has been proposed to depend on the constitution of these plasma membrane subdomains.[25] For example, a decrease in the levels of cholesterol promoted by treatment of cells with squalestatin results in a redistribution of PrP^C away from Triton X-100 insoluble lipid rafts and was reversed by addition of soluble cholesterol.[21] Based on these observations, we hypothesize that prion replication may result in localized alteration of the molecular composition of the lipid rafts in which PrP replication is occurring, and this leads to a local reduction or exclusion of proteins such as caveolin 1 and synaptophysin from this subset of lipid rafts, while having no effect on the proteins resident in neighboring rafts. This would explain why a proportion of caveolin 1 and synaptophysin shift to more dense fractions of the sucrose gradient, whereas other proteins such as Thy-1 are unaffected. Loss of proteins such as caveolin 1 and synaptophysin from the lipid raft fraction would thus be an early event in the breakdown of neuronal signaling and synaptic function. We are currently performing a more detailed analysis of the composition of PrP^{res}-containing DRMs during the course of the disease, to address some of these issues.

In summary we show that the presence of PrP^{res} in DRMs occurs at early stages of the progression of

scrapie in mouse in cell bodies and axons. This was not associated with alterations in the biochemical properties of these membrane subdomains. In parallel, caveolin 1 and synaptophysin, two DRM-resident proteins that interact normally with PrP^{C} and play a role in synaptic function, were found in non-DRM fractions in both neuronal compartments. These changes were observed before a decrease in the number of cell bodies that was only seen at advanced stages of scrapie. We propose that the conversion of PrP^{c} into PrP^{res} alters the association of proteins, such as caveolin 1 and synaptophysin, related to synaptic function within DRMs. This results in progressive neuronal dysfunction contributing to neuronal death and clinical signs at advanced stages of prion diseases.

Acknowledgment

We thank Elizabeth Vial for technical assistance.

References

1. Collinge J: Prion diseases of humans and animals: their causes and molecular basis. Annu Rev Neurosci 2001, 24:519–550
2. Johnson RT, Gibbs Jr CJ: Creutzfeldt-Jakob disease and related transmissible spongiform encephalopathies. N Engl J Med 1998, 339:1994–2004
3. Prusiner SB: Prions. Proc Natl Acad Sci USA 1998, 95:13363–13383
4. Borchelt DR, Taraboulos A, Prusiner SB: Evidence for synthesis of scrapie prion proteins in the endocytic pathway. J Biol Chem 1992, 267:16188–16199
5. Caughey B, Raymond GJ, Ernst D, Race RE: N-terminal truncation of the scrapie-associated form of PrP by lysosomal protease(s): implications regarding the site of conversion of PrP to the protease-resistant state. J Virol 1991, 65:6597–6603
6. Vey M, Pilkuhn S, Wille H, Nixon R, DeArmond SJ, Smart EJ, Anderson RG, Taraboulos A, Prusiner SB: Subcellular colocalization of the cellular and scrapie prion proteins in caveolae-like membranous domains. Proc Natl Acad Sci USA 1996, 93:14945–14949
7. Jeffrey M, Goodsir CM, Bruce ME, McBride PA, Fraser JR: In vivo toxicity of prion protein in murine scrapie: ultrastructural and immunogold studies. Neuropathol Appl Neurobiol 1997, 23:93–101
8. Simons K, Toomre D: Lipid rafts and signal transduction. Nat Rev Mol Cell Biol 2000, 1:31–39
9. Naslavsky N, Stein R, Yanai A, Friedlander G, Taraboulos A: Characterization of detergent-insoluble complexes containing the cellular prion protein and its scrapie isoform. J Biol Chem 1997, 272:6324–6331
10. Tsui-Pierchala BA, Encinas M, Milbrandt J, Johnson EM: Lipid rafts in neuronal signaling and function. Trends Neurosci 2002, 25:412–417
11. Mouillet-Richard S, Ermonval M, Chebassier C, Laplanche JL, Lehmann S, Launay JM, Kellermann O: Signal transduction through prion protein. Science 2000, 289:1925–1928
12. Hetz C, Maundrell K, Soto C: Is loss of function of the prion protein the cause of prion disorders? Trends Mol Med 2003, 9:237–243
13. Martins VR, Linden R, Prado MA, Walz R, Sakamoto AC, Izquierdo I, Brentani RR: Cellular prion protein: on the road for functions. FEBS Lett 2002, 512:25–28
14. Hetz C, Soto C: Protein misfolding and disease: the case of prion disorders. Cell Mol Life Sci 2003, 60:133–143
15. Hetz C, Russelakis-Carneiro M, Maundrell K, Castilla J, Soto C: Caspase-12 and endoplasmic reticulum stress mediate neurotoxicity of pathological prion protein. EMBO J 2003, 22:5435–5445
16. Cunningham C, Deacon R, Wells H, Boche D, Waters S, Diniz CP, Scott H, Rawlins JN, Perry VH: Synaptic changes characterize early behavioural signs in the ME7 model of murine prion disease. Eur J Neurosci 2003, 17:2147–2155
17. Siso S, Puig B, Varea R, Vidal E, Acin C, Prinz M, Montrasio F, Badiola J, Aguzzi A, Pumarola M, Ferrer I: Abnormal synaptic protein expression and cell death in murine scrapie. Acta Neuropathol (Berl) 2002, 103:615–626
18. Ferrer I: Synaptic pathology and cell death in the cerebellum in Creutzfeldt-Jakob disease. Cerebellum 2002, 1:213–222
19. Naslavsky N, Shmeeda H, Friedlander G, Yanai A, Futerman AH, Barenholz Y, Taraboulos A: Sphingolipid depletion increases formation of the scrapie prion protein in neuroblastoma cells infected with prions. J Biol Chem 1999, 274:20763–20771
20. Taraboulos A, Scott M, Semenov A, Avrahami D, Laszlo L, Prusiner SB, Avraham D: Cholesterol depletion and modification of COOH-terminal targeting sequence of the prion protein inhibit formation of the scrapie isoform. J Cell Biol 1995, 129:121–132
21. Bate C, Salmona M, Diomede L, Williams A: Squalestatin cures prion-infected neurons and protects against prion neurotoxicity. J Biol Chem 2004, 279:14983–14990
22. Baron GS, Wehrly K, Dorward DW, Chesebro B, Caughey B: Conversion of raft associated prion protein to the protease-resistant state requires insertion of PrP-res (PrP(Sc)) into contiguous membranes. EMBO J 2002, 21:1031–1040
23. Perry VH: Evidence for an amacrine cell system in the ganglion cell layer of the rat retina. Neuroscience 1981, 6:931–944
24. Russelakis-Carneiro M, Saborio GP, Anderes L, Soto C: Changes in the glycosylation pattern of prion protein in murine scrapie. Implications for the mechanism of neurodegeneration in prion diseases. J Biol Chem 2002, 277:36872–36877
25. Simons K, Ehehalt R: Cholesterol, lipid rafts, and disease. J Clin Invest 2002, 110:597–603
26. Galbiati F, Razani B, Lisanti MP: Emerging themes in lipid rafts and caveolae. Cell 2001, 106:403–411
27. Harmey JH, Doyle D, Brown V, Rogers MS: The cellular isoform of the prion protein, PrPc, is associated with caveolae in mouse neuroblastoma (N2a) cells. Biochem Biophys Res Commun 1995, 210:753–759
28. Hannah MJ, Schmidt AA, Huttner WB: Synaptic vesicle biogenesis. Annu Rev Cell Dev Biol 1999, 15:733–798
29. Jeffrey M, Halliday WG, Bell J, Johnston AR, MacLeod NK, Ingham C, Sayers AR, Brown DA, Fraser JR: Synapse loss associated with abnormal PrP precedes neuronal degeneration in the scrapie-infected murine hippocampus. Neuropathol Appl Neurobiol 2000, 26:41–54
30. Linden R, Perry VH: Massive retinotectal projection in rats. Brain Res 1983, 272:145–149
31. Fraser H: Neuronal spread of scrapie agent and targeting of lesions within the retino-tectal pathway. Nature 1982, 295:149–150
32. Kurzchalia TV, Parton RG: Membrane microdomains and caveolae. Curr Opin Cell Biol 1999, 11:424–431
33. Braun JE, Madison DV: A novel SNAP25-caveolin complex correlates with the onset of persistent synaptic potentiation. J Neurosci 2000, 20:5997–6006
34. Lledo PM, Tremblay P, DeArmond SJ, Prusiner SB, Nicoll RA: Mice deficient for prion protein exhibit normal neuronal excitability and synaptic transmission in the hippocampus. Proc Natl Acad Sci USA 1996, 93:2403–2407
35. Wong K, Qiu Y, Hyun W, Nixon R, VanCleff J, Sanchez-Salazar J, Prusiner SB, DeArmond SJ: Decreased receptor-mediated calcium response in prion-infected cells correlates with decreased membrane fluidity and IP3 release. Neurology 1996, 47:741–750
36. Guan Z, Soderberg M, Sindelar P, Prusiner SB, Kristensson K, Dallner G: Lipid composition in scrapie-infected mouse brain: prion infection increases the levels of dolichyl phosphate and ubiquinone. J Neurochem 1996, 66:277–285
37. Brugger B, Graham C, Leibrecht I, Mombelli E, Jen A, Wieland F, Morris R: The membrane domains occupied by glycosylphosphatidylinositol-anchored prion protein and Thy-1 differ in lipid composition. J Biol Chem 2004, 279:7530–7536
38. Botto L, Masserini M, Cassetti A, Palestini P: Immunoseparation of prion protein-enriched domains from other detergent-resistant membrane fractions, isolated from neuronal cells. FEBS Lett 2004, 557:143–147